Proposal of Fast and High-Precision Control for Ball-Screw-Driven Stage by Explicitly Considering Elastic Deformation

Hongzhong Zhu
Department of Electrical Engineering
Graduate School of Engineering
The University of Tokyo
Tokyo, Japan 113–8656
Email: zhu@hflab.k.u-tokyo.ac.jp

Hiroshi Fujimoto
Department of Electrical Engineering
Graduate School of Engineering
The University of Tokyo
Tokyo, Japan 113–8656
Email: fujimoto@k.u-tokyo.ac.jp

***Abstract*—Ball-screw-driven stages are extensively used in industry for long-range and high-precision fabrication thanks to their high efficiency and high ability to apply/withstand high thrust loads. However, spring-like nonlinear friction in zero-speed region significantly affects the control performance. In this paper, the mechanical deformation characteristics at zero-speed point after low deceleration and after high deceleration are analyzed. It is found that the mechanical deformation characteristic of fast motions differs from the case of slow motions in zero-speed region, and therefore performing friction compensation should take the motion conditions into account. Then, after introducing a variable to evaluate the elastic deformation of the total mechanical components, a novel friction compensation method for fast reverse motions using Sigmoid function is proposed to enhance the control performance by explicitly considering the elastic deformation. Finally, Experiments are performed to verify the effectiveness of the proposed method.**

I. Introduction

Ball screws are widely used in industry to position stages and cutting tools to the desired locations; hence their positioning speed and accuracy determine the quality and productivity of manufactures. One disadvantage of a ball screw is that the rotary inertia makes it difficult to achieve high accelerations using a motor of a given size [1], [2]. A second, still need to be conqued, nonlinear mechanical deformation during the deceleration/acceleration limits the motion performance. Especially, the nonlinear friction derived from the mechanical deformation, named as rolling friction, becomes a deterministic disturbance and significantly degrades the trajectory tracking performance in zero-speed region [3], [4], [7]–[9], [15].

Rolling friction has the hysteretic property caused by micro-slip loss or plastic deformation within contact interface. Much research in the literature focuses on building precise friction models to depict the friction characteristics of ball-screw-driven stages. Among them, Hsieh and Pan proposed a model that expresses the hysteretic feature as a combination of a plastic module and a nonlinear spring module [5]. Swevers *et al.* presented a complete and accurate model to describe the hysteresis characteristics of the friction using some mathematical equations [13]. These models are so complex that not only the identification of the parameters but also the implementation to the real systems are a time-consuming work. In order to take more priority over the ease of implementation, a heuristic friction model, which is also referred to as the Generalized Maxwell-Slip Model (GMS), was proposed in [14]. However, the large number of parameters, which are required to be carefully identified, would increase the cost in design and maintenance. Moreover, the friction compensation law of these methods may not suit for practical situations where the motion conditions, i.e., fast reverse motions, are different with the motion conditions in friction identification. This viewpoint will be clarified in next sections that the conventional compensation law cannot perfectly compensate nonlinear friction in fast reverse motions and non-reverse motions.

Another well known method for suppressing nonlinear friction is disturbance observer [6], [12], [16]. The method can theoretically nominalize the control plant so that the performance can be significantly improved. However, due to the limited bandwidth for disturbance rejection and the inaccuracy of velocity signals at low speed, nonlinear friction cannot be completely reduced in zero-speed region. Because of these reasons, disturbance observer and friction compensator coexist in many proposed methods [9], [10], [16].

In order to obtain a better friction compensation, mechanical deformation analysis of different motion conditions becomes important. Motivated by this observation, the elastic deformation characteristics of a ball-screw-driven stage at zero-speed point after high deceleration motions as well as after low deceleration motions are explored. Then, a novel friction compensation method is proposed for fast reverse motions. The models are very simple so that the identification of the parameters and the implementation of the compensation laws can be simplified. These points are very important in real situations since the maintenance also becomes easy.

The remainder of this study is organized as follows. Section II described the experimental setup and problem description. Section III analyzes the deformation characteristics of ball-screw stage in the zero-speed region. A friction compensation approach based on Sigmoid function for the fast reverse motions is proposed in Section IV. Experiments are performed to show the applicability of the proposed approach in Section V. The conclusion is summarized in Section VI.

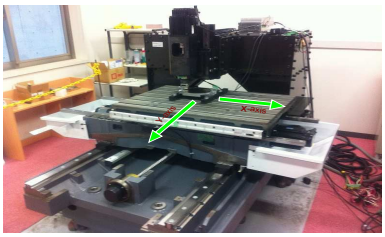

Fig. 1. Experimental device.

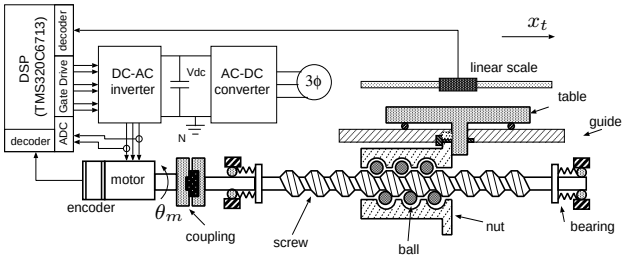

Fig. 2. Configuration of ball-screw-driven stage in X-axis direction.

II. Experimental System and Problem Description

A. Experimental setup

Fig. 1 shows the overview of an experimental XY ball-screw-driven stage. The configuration of X-axis stage is shown in Fig. 2. Here, x_t and θ_m are the table position and the rotation angular of the motor, respectively. Table. I shows the parameters of the stage in X-axis direction. Ball screw is directly connected with the shaft of a PM motor through coupling. The servo motor is equipped with an absolute encoder whose resolution is 2^{20} pulses/rev. A linear scale with a resolution of $100\mathrm{nm}$ is applied to measure the table position. Current vector control method is exploited to control the servo motor, and the bandwidth of the current method is 1kHz. The frequency characteristics of the experimental stage from torque to motor angular position and from torque to table position are shown by the solid line in Fig. 3. The rigid model of the stage from torque to motor angular position is expressed by

$$P_{u\theta}(s) = \frac{1}{J_n s^2 + B_n s}, \tag{1}$$

where $J_n = 2.6 \times 10^{-3}\,\mathrm{kgm}^2$ is the equivalent moment of inertia and $B_n = 0.070\,\mathrm{Nms/rad}$ is the equivalent viscous friction coefficient. The nominal transfer function from torque

TABLE I. Parameters of the stage in X-axis direction

motor inertia moment J_m	2.300×10^{-3} kgm^2
motor viscosity coefficient B_m	1.177 Nms/rad
torque constant K_τ	0.715 Nm/A
length of ball screw L_b	1.169 m
mass of ball screw M_b	9.353 kg
viscosity coefficient of ball screw B_b	5.000×10^{-2} Nms/rad
rotation-to-translation ratio R	1.910 mm/rad
mass of table M_t	273.0 kg
viscosity coefficient of linear guide C_t	1.000×10^{4} Ns/m

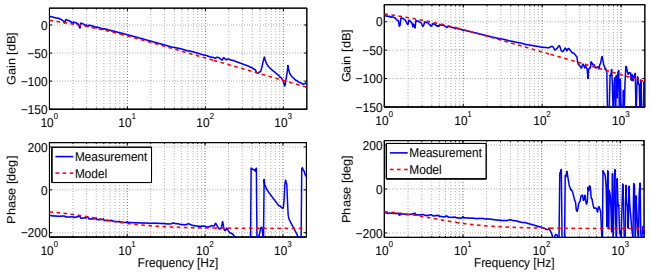

(a) (b)

Fig. 3. Frequency response of the stage. (a) Torque to motor position θ_m; (b) Torque to table position x_t.

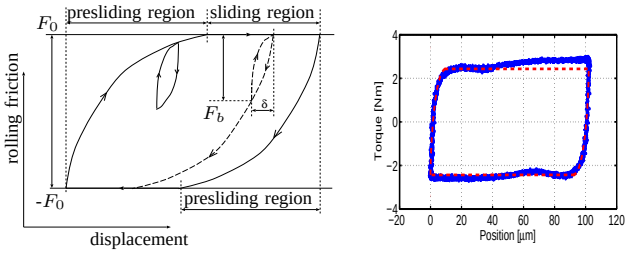

(a) Rolling friction characteristic. (b) Experimental data and model of friction.

Fig. 4. Rolling friction characteristic and experimental measurement.

to table position is

$$P_{ux}(s) = RP_{u\theta} = \frac{R}{J_n s^2 + B_n s}. \tag{2}$$

Here, R is the rotation-to-translation ratio of the screw. The models are shown by the dashed line in Fig. 3.

A conceptual characteristic of rolling friction is shown in Fig. 4(a). The rolling friction consists of presliding region where the rolling balls can not roll perfectly due to the deformation/slips at solid contact points in the grooves, and sliding region where rolling balls roll normally so that the friction behaves as the Coulomb friction. Here, x_s denotes the pre-sliding regime and F_0 is the Coulomb friction. Usually, the nonlinear friction of a real system is obtained by applying some very small periodic trajectory reference to the feedback control system and plotting the relationship between control input and stage position. The measured friction of the experimental stage in X-axis direction is shown in Fig. 4(b) by applying a small sinusoidal signal whose amplitude is $50\mu m$ and frequency is $0.05\mathrm{Hz}$. From the result, it is observed that the presliding region of the experimental device is about $15\mu m$. The dashed line in Fig. 4(b) shows the friction model using conventional GMS method [14].

B. Control system

A two-degree-of-freedom controller, an inverse-model-based disturbance observer (DOB) and feedforward friction compensation are designed for the plant. The block diagram of

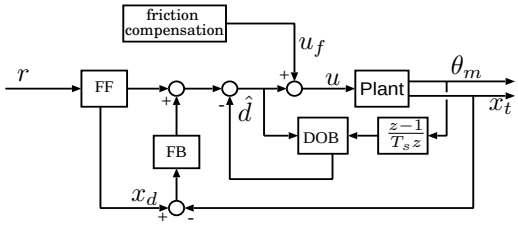

Fig. 5. Block diagram of control system with two-degree-of-freedom controller, an inverse-model-based disturbance observer and feedforward friction compensation.

control system is shown in Fig. 5. r is the trajectory reference, and u is the control input. The feedforward controller is designed as the stable inverse system of the nominal plant (2) via Perfect tracking control (PTC) [17]. It is proved that the perfect tracking at every sampling instant can be theoretically guaranteed. x_d is the desired reference generated by the PTC. A PID compensator, designed by pole assignment approach, is applied as the feedback controller to regulate the table position x_t. The resulting bandwidth of the closed loop is $20\mathrm{Hz}$. In addition, an inverse-model-based disturbance observer is designed to nominalize the plant using motor angular position θ_m. A 1^{st}-order low-pass filter whose bandwidth is $80\mathrm{Hz}$ is applied for DOB, and the estimated disturbance is denoted as $\hat{d}$. Note that the rotation angular of motor θ_m, not the stage position, is used for DOB in order to obtain a higher bandwidth for disturbance rejection. Feedforward friction compensation is considered in this study and the design will be introduced in Section IV. DSP(TMS320C6713, 225MHz) is used as the processor to implement the control system. The PID compensator, DOB and friction compensation are discretized by $0.5\mathrm{ms}$, and the sampling period for PTC is $1\mathrm{ms}$.

C. Problem description

Conventional friction compensation methods treat the friction as a springlike friction having the hysteretic characteristics shown in Fig. 4(a). The conventional friction compensation methods compensate the friction from the reverse point without considering the mechanical deformation before the reverse. In practical situation, this neglected deformation state plays a dominant role in the performance degradation. It will be illustrated that the elastic deformation pattern after low deceleration is different with the one after high deceleration. It is the difference that makes the conventional compensation approach not work well in fast reverse motions. An example is shown in Fig. 6(a) and Fig. 6(b). In both experiments, friction compensation was performed using the GMS method [14]. It is observed that the compensation performance is significantly degraded in the fast reverse motion. In the next section, the elastic deformation characteristics in zero-speed region is studied in detail.

III. Deformation Characteristics in Zero-Speed Region

A. Modeling of ball-screw-driven stage

The force analysis of nut and its model are shown in Fig. 7. The balls between nut and screw are regarded as nonlinear springs. Here, F_t denotes the counteracting force from the

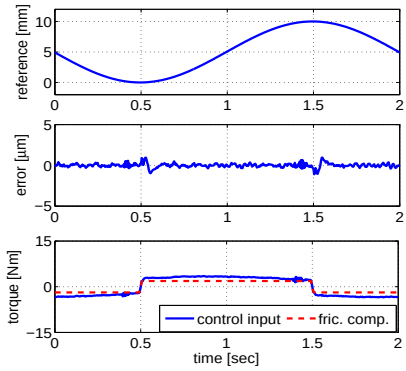

(a) Tracking performance of a sinusoidal trajectory with small amplitude with conventional friction compensation.

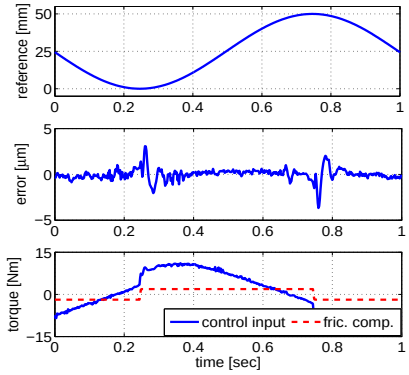

(b) Tracking performance of a sinusoidal trajectory with large amplitude with conventional friction compensation.

Fig. 6. Experimental trajectory tracking results. The upper graphs show the trajectory references, middle graphs show the trajectory tracking errors, and the lower graphs show the input torques/friction compensation signals.

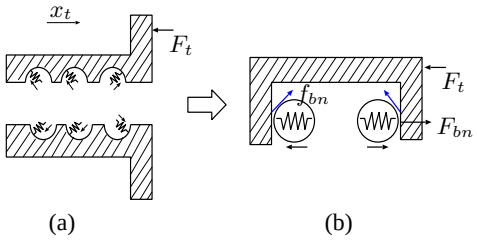

Fig. 7. (a) Force analysis of nut and (b) the model.

table, f_{bn} denotes the friction between the balls and nut, and F_{bn} is the drive force or the braking force from the screw to the nut in the motion direction. The forces in Z-axis direction is ignored in the model since they are balanced.

Based on this analysis, the ball-screw-driven stage is modeled as Fig. 8. For simplicity, the stiffness between the nut and the table is supposed to be very large so that the body consisting of the nut and the table is rigid. M denotes the total mass of nut and table. f_g denotes the friction of guide way. In

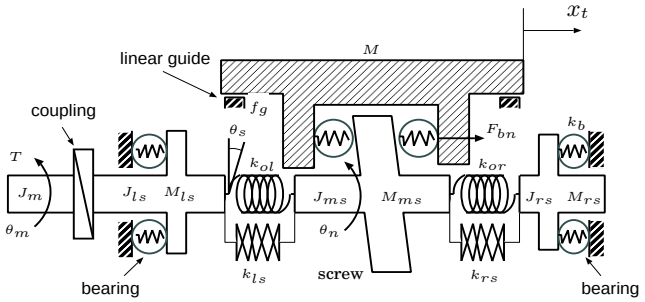

Fig. 8. Mechanical model of the ball screw drive system.

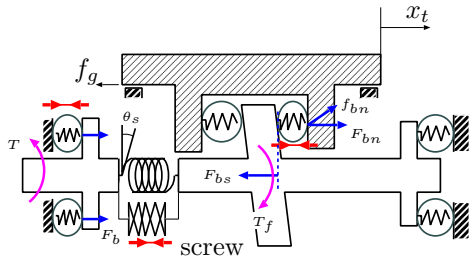

Fig. 9. Elastic deformation during low deceleration. Right-hand side of the grooves of the nut, left part of the screw, and the bearings at the left-hand side of the screw are compressed. This pattern is denoted as *Pattern I*.

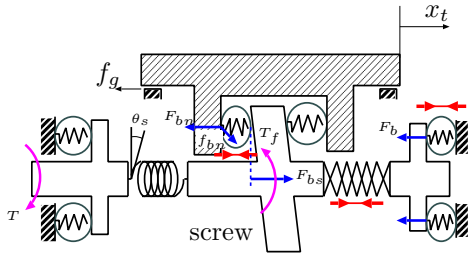

Fig. 10. Elastic deformation during high deceleration. Left-hand side of the grooves of the nut, right part of the screw, and the bearings at the right-hand side are compressed. This pattern is denoted as *Pattern II*.

order to analyze the deformation of mechanical components in more detail, the screw is divided into left part, middle part and right part, and the inertia/mass of each part is denoted by J_{xs}/M_{xs} where the subscript x stands for l, m or r, as shown in Fig. 8. k_{ol} and k_{or} are the torsional stiffness of the screw between the end sides of screw and the nut, and k_{ls} and k_{rs} are the axial stiffness of the screw. θ_s is the rotational displacement of the screw which is defined by

$$\theta_s := \theta_m - \theta_n, \tag{3}$$

where θ_n is the rotation angle of the screw at the center of the nut. Suppose that the friction of the bearing at the right side of the screw is small so that the torsional displacement at the right part of screw is ignored.

B. Deformation patterns at the zero-speed point

For ease of analysis, the initial deformations of the mechanical components caused by the preloads which are applied on the nut and screw are neglected. The motion equation of the linear part including the nut and the table can be expressed by

$$M\ddot{x}_t = F_{bn} - f_g. \tag{4}$$

According to the direction of F_{bn}, there are two possible cases during the deceleration.

1) F_{bn} has the same direction with the motion direction in the deceleration: In this case, the deceleration is low so that F_{bn} is required to work as drive force to balance out the guide friction f_g. During the deceleration until the stage stops, the counteracting force of F_{bn}, which is denoted by F_{bs}, acts on the screw. F_{bs} needs to be balanced out by the supporting force F_b generated by the bearings located at the left-hand side of the screw. Therefore, the deformation characteristic of the screw-ball-nut at zero speed can be illustrated in Fig. 9. Here, T_f is the torque generated by the friction between rolling balls and grooves of the screw. During the deceleration motion, the bearing on the left-hand side, the left part of the screw and the right-hand side of the grooves of the nut are compressed, as indicated by the icon of two arrows in counter direction in the figure. In addition, the torsion deformation θ_s is positive in this case by the definition (3). For convenience, the deformation shown in Fig. 9 is denoted as *Pattern I*.

2) F_{bn} is in the opposite direction with the motion direction in the deceleration: In this case, the deceleration is high so that the friction f_g is not enough to brake the stage, and F_{bn} is required to work as a braking force to have the stage track a given trajectory reference. In this case, F_{bs}, F_b, T_f and T also change their directions, as shown in Fig. 10. Therefore, the bearing on the right-hand side, the right part of the screw and the left-and side of the grooves of the nut are compressed in this deceleration motion. The torsion deformation θ_s is negative in this case. This deformation is denoted as *Pattern II*.

Due to the different deformation patterns at zero-speed point, the friction property of the coming acceleration motions also vary greatly from each other.

In the acceleration after the reverse, F_{bn} is required to balance out f_g as well as to accelerate the stage in the opposite direction after the stage is stopped. Therefore, the left-hand side of the grooves of the nut, the right part of the screw and the bearing at the right-hand side need to be compressed to generate F_{bn}, which is actually the *Pattern II* shown in Fig. 10. It is found that the elastic deformation should be shifted from *Pattern I* to *Pattern II* in slow reverse motions. However, the deformation pattern is not changed in fast reverse motions. Note that the motion for identifying nonlinear friction of a real ball-screw-driven stages is a slow reverse motion. Therefore, the identified friction model is not suitable for the fast reverse motions since the deformation pattern is different.

In the case of non-reverse motion where the coming acceleration motion is in the same direction with the deceleration. F_{bn} works as the driven force in the acceleration. In this case, the right-hand side of grooves of the nut, the left part of the screw and the bearing at the left-hand side need to be compressed to generate F_{bn}, which is the *Pattern I* shown in Fig. 9. Therefore, the elastic deformation pattern is not changed in the case of slow non-reverse motions, while it is changed from *Pattern II* to *Pattern I* in fast non-reverse motions.

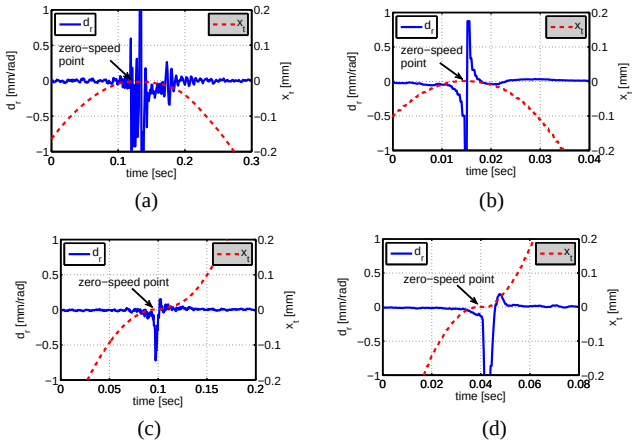

Fig. 11. Comparison of l_d of four cases. (a): Slow reverse motion; (b): Fast reverse motion; (c): slow non-reverse motion; (d): fast non-reverse motion.

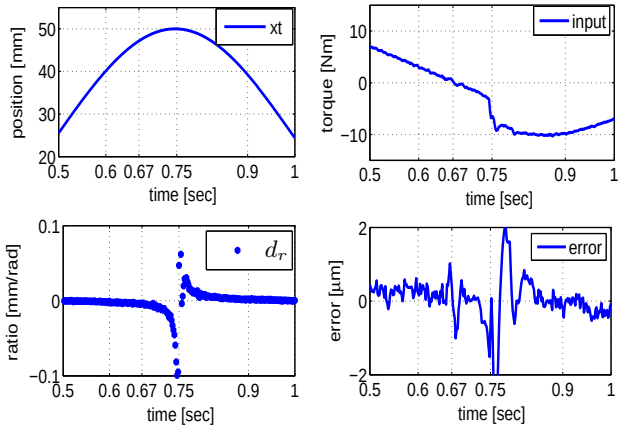

Fig. 12. Details of the fast reverse motion shown in Fig. 6(b). The upper left graph is the position of stage, the lower left graph is the deformation ratio d_r, the upper right graph is the control input and the lower right graph is the position tracking error.

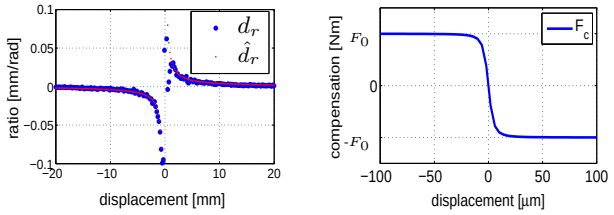

Fig. 13. (a) Comparison of d_r and its estimation $\hat{d}_r$; (b) Compensation law in the case of fast reverse motion where the velocity changes from negative to positive.

C. Evaluation of mechanical deformation

In order to evaluate the elastic deformations, a variable is defined as follows:

$$l_d := \frac{\frac{d\,x_t}{d\,t}}{\frac{d\,\theta_m}{d\,t}} = \frac{d\,x_t}{d\,\theta_m}. \tag{5}$$

For discrete-time realization, the following approximation is performed:

$$l_d = \frac{d\,x_t}{d\,\theta_m} \approx \frac{\Delta x_t}{\Delta \theta_m} = \frac{x_t[k] - x_t[k-p]}{\theta_m[k] - \theta_m[k-p]}. \tag{6}$$

Here, Δx_t and $\Delta \theta_m$ are the position/angular displacement in a given $p+1$ sampling periods, and k is the current time index. In the ideal case without elastic deformation, l_d is the same with the rotation-to-translation ratio R of the screw. However, because of the dynamic deformation of the mechanical components, l_d varies when the drive force or cutting force fluctuates, especially in the zero-speed region. For convenience, the deformation ratio is defined as

$$d_r = l_d - R. \tag{7}$$

Experimental results of four cases of slow reverse motion, fast reverse motion, slow non-reverse motion and fast non-reverse motion are shown in Fig. 11. In the figure, the dashed lines show the position signals of the table x_t and the solid lines show the variation of d_rs. In the cases of fast reversal/non-reverse motions, it is shown that d_r gradually reduced before the stage stops. On the other hand, in the cases of slow reversal/non-reverse motions, though d_r cannot be accurately calculated due to the position measurement errors, it can also be found that the nominal value of d_r almost remains constant until the stage stops.

In order to obtain precise friction compensation in zero-speed region, the deformation characteristics should be taken into account. In the following, a novel torque compensation method for fast reverse motions is presented.

IV. Friction Compensation for Fast Reverse Motions

As analyzed in Section III, the deformation characteristics of fast reverse motions differ from the characteristics of the slow reverse motion used for friction identification. Hence, the friction compensation for fast reverse motions using the rolling friction model Fig. 4(a) cannot obtain the same performance as the case of slow reverse motions, as shown in Fig. 6(b). The details during the reverse are shown in Fig. 12. It is observed that when the control input changes its direction at $t = 0.67\,s$, the mechanical deformation changes its pattern from *Pattern I* to *Pattern II* so that the control performance is degraded. In addition, the control performance has already been remarkably degraded before the reverse that happens at $t = 0.75\,s$. Along with the performance degradation, the mechanical deformation, which is evaluated by d_r, also changes rapidly. Therefore, utilizing the information inherent in d_r to enhance the braking effects before the reverse and compensate the nonlinear friction after the reverse becomes possible.

For analysis, d_r is regarded as a power function

$$\hat{d}_r = \sigma z^{-1}, \tag{8}$$

where z is the displacement from the reversal point, and σ is

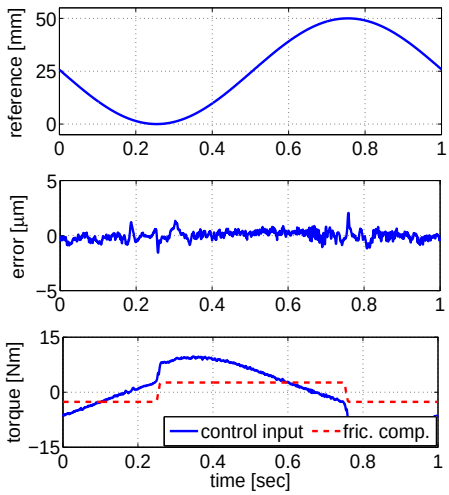

Fig. 14. Experimental results of the fast reverse motion by proposed method.

a factor. The comparison of d_r and $\hat{d}_r$ is shown in Fig. 13(a), where $\sigma = 0.04$ when z is measured in unit of millimeter.

In order to enhance the braking effects before the reverse and compensate the nonlinear friction after the reverse, the following torque compensation law using Sigmoid function is applied:

$$F_c = \text{sgn}(v_t)\sqrt{\frac{(\gamma/\hat{d}_r)^2}{1+(\gamma/\hat{d}_r)^2}}\,F_0. \tag{9}$$

Here, v_t is the velocity of stage and $\text{sgn}(v_t)$ is the sign of v_t. γ is a parameter that depends on the axial stiffness and the torsional stiffness of the ball-screw-driven stage. The compensation law is demonstrated in Fig. 13(b) when the motion direction is from positive to negative. In real implementation, the design of σ and γ can be considered together to let F_c vary from F_0 to $-F_0$ mainly in $[-x_s/2 \;\; x_s/2]$.

V. Experiments

A sine signal $x_t^*(t) = 25(1-\cos(2\pi t))$mm whose maximum deceleration is $100\pi^2$mm/s^2 is applied as the trajectory reference to evaluate the friction compensation performance. For the experimental device shown in Section II, this trajectory in the zero-speed region can be regarded as fast reverse motion.

The experimental results using the proposed method are shown in Fig. 14. Compared to the results of conventional GMS method shown in Fig. 6(b), the maximum position tracking error is reduced about 44% from $3.68\,\mu$m to $2.05\,\mu$m. Therefore, the Sigmoid-function-based compensation method can remarkably improves the position tracking performance.

VI. Conclusion

In this study, the elastic deformation of mechanical components of experimental ball-screw-driven stage is analyzed in detail. It is obtained that the elastic deformation patterns at zero speed are different between the cases after low deceleration and the cases after high deceleration. In order to evaluate the dynamical deformation in the zero-speed region, a new variable is defined using the information of table position and motor angular. Then, a novel nonlinear compensation method based on Sigmoid function is proposed for fast reverse motion by explicitly considering the elastic deformation characteristics, and experiments are performed to verify the effectiveness.

Acknowledgment

This work was supported in part by the DMG MORI SEIKI Co. Ltd.. The authors gratefully acknowledge valuable suggestions from Shinji ISHII, Koji YAMAMOTO and Yuki TERADA from the DMG MORI SEIKI Co. Ltd..

References

[1] Y. Altintas, A. Verl, C. Brecher, L. Uriarte, and G. Pritschow, "Machine Tool Feed Drives", *Manufacturing Technology*, Vol. 60, pp. 779–796, 2011.

[2] K.K. Varanasi, and S.A. Nayfeh, "The Dynamics of Lead-Screw Drives: Low-Order Modeling and Experiments", *Trans. ASME, J. Dyn. Sys. Meas. Control*, Vol. 126, pp. 388–396, 2004.

[3] S. Fukada, B. Fang, and A. Shigeno, "Experimental Analysis and Simulation of Nonlinear Microscopic Behavior of Ball Screw Mechanism for Ultra-Presion Positioning", *Precision Engineering*, Vol. 35, pp. 650–668, 2011.

[4] Y. Maeda, and M. Iwasaki, "Initial Friction Compensation Using Rheology-Based Rolling Friction Model in Fast and Precise Positioning", *IEEE Trans. Ind. Electron.*, Vol. 60, No. 9, pp. 3865–3876, 2013.

[5] C. Hsieh, and Y.C. Pan, "Dynamic Behavior and Modelling of the Pre-sliding Static Friction", *Wear*, Vol. 242, pp. 1-17, 2000.

[6] W.S. Huang, C.W. Liu, P.L. Hsu, and S.S. Yeh, "Precision Control and Compensation of Servomotors and Machine Tools via the Disturbance Observer", in *IEEE Trans. Ind. Electro.* , Vol. 57, No. 1, pp. 420–429, 2010.

[7] F. Huo, and A.-N. Poo, "Precision Contouring Control of Machine Tools", *Int. J. Adv. Manuf. Technol.*, Vol. 64, pp. 319–333, 2013.

[8] M. Iwasaki, K. Seki, and Y. Maeda, High-Precision Motion Control Techniques–A Promising Approach to Improving Motion Performance, *IEEE Trans. Ind. Electron. Magazine*, Vol. 6, No. 1, pp.32-40, 2012.

[9] Z. Jamaludin, H. V. Brussel, and J. Swevers, Friction Compensation of an XY Feed Table Using Friction-Model-Based Feedforward and an Inverse-Model-Based Disturbance Observer, *IEEE Trans. Ind. Electron.* , Vol. 56, No. 10, 2009.

[10] H. S. Lee and M. Tomizuka, Robust Motion Controller Design for High-Accuracy Positioning Systems, *IEEE Trans. Indust. Electr.* , Vol. 43, No. 1, pp. 48–55, Feb. 1996.

[11] T. Umeno and Y. Hori, Robust Speed Control of DC Servomotors Using Modern Two Degree-of-Freedom Control Design, *IEEE Trans. Indust. Electr.* , Vol. 38, No. 5, pp. 363–368, Oct. 1991.

[12] S. Sakai and Y. Hori, Ultra-low Speed Control of Servomotor using Low Resolution Rotary Encoder, in *Proc. IECON 21st int. Conf. Ind. Electron.* , Orlando, FL, Vol. 1, pp. 615–620, 1995.

[13] J. Swevers, F. Al-Bender, C. G. Ganseman, and T. Prajogo, An integrated friction model structure with improved presliding behavior for accurate friction compensation, *IEEE Trans. Automat. Contr.*, Vol. 45, pp. 675–686, Apr. 2000.

[14] F. Al-Bender, V. Lampaert and J. Swevers, The Generalized Maxwell-Slip Model: A Novel Model for Friction Simulation and Compensation, *IEEE Trans. Autom. Control*, Vol. 50, No. 11, pp. 1883-1887, 2005.

[15] H. Zhu and H. Fujimoto, Proposal of Nonlinear Friction Compensation Approach for a Ball-Screw-Driven Stage in Zero-Speed Region including Non-Velocity-Reversal Motion, *IECON 2013*, to be presented.

[16] Y. Maeda, and M. Iwasaki, "Analytical Examinations and Compensation for Slow Settling Response in Precise Positioning Based on Rolling Friction Model", *Advanced Motion control* , pp. 24–29, Nagaoka, Mar. 2010.

[17] H. Fujimoto, Y. Hori, and A. Kawamura, Perfect Tracking Control based on Multirate Feedforward Control with Generalized Sampling Periods, *IEEE Trans. Ind. Electron.*, Vol. 48, No. 3, pp.636-644, 2001.